Hindawi
Complexity
Volume 2019, Article ID 9516865, 11 pages
https://doi.org/10.1155/2019/9516865

Research Article

Theoretical Study on Self-Organization of Vegetation Patterns Triggered by Water Resource in Deposited Sediment Layer

Tousheng Huang, Huayong Zhang, Zhao Liu, Ge Pan, Xiumin Zhang, and Zichun Gao

Research Center for Engineering Ecology and Nonlinear Science, North China Electric Power University, Beijing 102206, China

Correspondence should be addressed to Huayong Zhang; rceens@ncepu.edu.cn

Received 15 March 2019; Revised 29 May 2019; Accepted 16 June 2019; Published 4 July 2019

Academic Editor: Xiaopeng Zhao

This research focuses on the self-organization of vegetation patterns on severely degraded eroding lands, triggered by water resource in the deposited sediment layer on which the vegetation patterns are formed. A nonlinear spatiotemporal model is developed with the consideration of the interactions between vegetation biomass and water resource stored in the sediment layer. With employment of the model, the conditions for pattern formation of the considered ecological system are determined via Turing instability analysis. Numerical simulations of the research demonstrate the formation of banded, labyrinth, and gapped vegetation patterns, with the parameter values taken from the literature. The characteristics of the vegetation patterns are analyzed. Comparing the characteristics of the vegetation patterns of this research with that available in literature, great similarity of pattern formation is shown. The results obtained provide a theoretical comprehension on natural vegetation restoration of severely degraded eroding lands.

1. Introduction

The vegetation in semiarid and arid regions may hardly maintain homogeneous cover and often exhibit spectacular organized spatial patterns due to insufficiency of water resource [1–6]. As one type of important landscape widely distributed around the world, the spatial vegetation patterns self-organized in water-limited ecosystems have been studied a lot via empirical and theoretical manners [7–15].

Until now, the researchers have reached a consensus that a balance of interactions between vegetation biomass and water resource is the main process which results in vegetation pattern formation in the water-limited ecosystems [6, 10, 16]. The interactive mechanisms between biomass and water mainly reflect in two aspects. First, more vegetation biomass leads to increased infiltration and concentration of water resource. This brings water redistribution between vegetated areas and bare areas. Second, uptake of soil water by plant roots promotes vegetation growth. This results in depletion of soil water and plant competition for the water resource.

Many mathematical models have been established to investigate the vegetation pattern formation in water-limited ecosystems. Klausmeier [7] brought up a model of plant biomass and water, theoretically demonstrating the alternating bands of vegetation and bare ground on hillslopes. HilleRisLambers et al. [8] and Rietkerk et al. [9] developed a model of biomass, soil water, and surface water and predicted spotted, labyrinth, gapped, and striped patterns. von Hardenberg et al. [17] raised a model focusing on the ground water available to the plants and expounded the diversity of vegetation patterns along rainfall gradient. For understanding and revealing the nonlinear characteristics of vegetation-water dynamics in the models, tools of theoretical analysis and numerical simulations are both effective and necessary [18–20]. For example, the vegetation pattern selection of the Klausmeier model was further investigated by standard multiple-scale analysis, revealing rich pattern structures including spotted, mixed, and stripe patterns in the arid flat environment [18]. Sun et al. also explored the model of von Hardenberg with the application of bifurcation analysis and amplitude equations and found a close relationship among feedback intensity, rainfall, and pattern dynamics of the vegetation [20].

However, a crucial condition is not often mentioned in the previous studies of vegetation pattern formation. It is that the topsoil layer may provide an environment of

water storage, vegetation establishment, and the interactions between water and biomass [21]. In some extreme situations, the available soil layer may disappear due to severe degradation of the land. For example, soil erosion may remove soil and destroy the soil layer [22–25]. Furthermore, the ground surface may be sealed by a soil crust such that the surface water can hardly infiltrate and therefore the living of plants cannot be supported [26–29]. In these extreme situations, a new interface which triggers the ecological processes of vegetation pattern formation needs to be discussed.

An important instance for such extreme cases is the vegetation pattern formation described by Bryan and Oostwoud Wijdenes [30]. They found that sequential scour and deposition favored the development of small-scale vegetation bands on low-angle alluvio-lacustrine flats surrounding Lake Baringo in the northern part of the Rift Valley, Kenya. As described by Bryan and Oostwoud Wijdenes [30] and Bryan and Brun [31], several centimeters of loose coarser soil were deposited on top of crusted, compact soil in depositional zones. Due to the higher infiltration and moisture storage, in comparing with that in the crusted soil surface, depositional zones could remain moist after rainstorms and support development of low ground vegetation. Consequently, typical vegetation bands could be found at many locations on the flats, extending for many meters in the crenulate lines along the contours of the land.

According to the findings described in literature [30], the water resource in deposited sediment layer can be considered as an important ecological factor which supports vegetation growth and triggers vegetation pattern formation. However, theoretically modeling studies of vegetation pattern formation in such case are still barely documented. In this research, a nonlinear spatiotemporal model is developed on the basis of the interactions between vegetation biomass and the water resource in the deposited layer. Through mathematical analysis and numerical simulations on the model, various vegetation patterns are found and shown. Different from many former works, the patterned vegetation of this research implies recovery of severely degraded ecosystems under water-limited condition.

2. Model Development

In 1999, Klausmeier established a nonlinear spatiotemporal model, fantastically interpreting the self-organization and maintenance of striped vegetation patterns in semiarid regions [7]. The vegetation pattern formation in the approach of Klausmeier [7] emerges in the case where the soil layer is scarcely disturbed and it merely involves the interactions between water resource and vegetation biomass. However, referring to Bryan and Oostwoud Wijdenes [30], Bryan and Brun [31], and Puigdefabregas et al. [32], the vegetation pattern formation can occur on low angle, smooth slopes over soils of high erodibility but low permeability. In other words, the disturbance of soil layer can be an important factor which determines the vegetation pattern formation.

As described in Bryan and Oostwoud Wijdenes [30] and Bryan and Brun [31], the pattern formation happens on severely degraded soil surface. On the one hand, soil erosion destroyed the topsoil layer, leaving eroded ground with sealed soil surface. On the other hand, the sediment layer deposited on the degraded ground provided living environments for plants. Similarly as described in Puigdefabregas et al. [32], the redistribution of the sediments posed great influences on the formation of vegetation patterns.

In such cases, the redistribution of sediments is regarded as the main factor which triggers the vegetation pattern formation. Since almost all of the water resource exists in the deposited sediment layer, the redistribution of sediments dominates the redistribution of water resource in such ecological systems. Accordingly, the spatial distribution of vegetation is controlled by the redistribution of sediments [32]. When the interactions between the vegetation and the redistribution of sediment water reach a balance, it indicates the possible formation of stable vegetation patterns.

Based on the above description and the field findings recorded in literature [30], we consider the water resource in the deposited sediment layer as an important ecological factor which supports vegetation growth and triggers vegetation pattern formation. According to this consideration, the Klausmeier model is modified. First, the available water resource for vegetation growth is provided by the water which exists in the deposited sediment layer. It is presumed that the supply of water resource into the ecological system is synchronized to the sediment deposition process. Second, the water movement is divided into two aspects, the movement of sediments along hillslopes and the lateral movement of water in the deposited sediment layer.

In the modified model, we introduce a new variable, which is the water resource in the deposited sediment layer, also briefly called sediment water below, denoted by S. And the other variable, plant biomass, is denoted by V. Therefore, the system of plant biomass and sediment water can be expressed by the following nonlinear partial differential equations:

$$\frac{\partial S}{\partial T} = A\left(1 - \frac{S}{S_m}\right) - LS - PSV^2 + U\frac{\partial S}{\partial X} + D_S\left(\frac{\partial^2 S}{\partial X^2} + \frac{\partial^2 S}{\partial Y^2}\right), \tag{1a}$$

$$\frac{\partial V}{\partial T} = HPSV^2 - MV + D_V\left(\frac{\partial^2 V}{\partial X^2} + \frac{\partial^2 V}{\partial Y^2}\right), \tag{1b}$$

in which T is time and X and Y are space; $A(1\text{-}S/S_m)$ describes the growth of the sediment layer as well as the sediment water; A is the maximal growth rate at $S = 0$ and S_m is the maximal thickness of the sediment water or deposited sediment layer; L is the evaporation rate of the sediment water; P describes the rate of per unit plant biomass taking up water; H expresses the conversion rate of plant biomass per unit water consumed; M is the mortality rate of plant biomass; $U\partial S/\partial x$ describes the downslope flux of sediments, and $D_S(\partial^2 S/\partial x^2 + \partial^2 S/\partial y^2)$ describes the lateral diffusion of the water in the sediments, just like the movement of soil water described by HilleRisLambers et al. [8] and Rietkerk et al. [9]; U and D_S are corresponding coefficients; D_V is the

Table 1: Interpretation of the symbols used in (1a) and (1b).

Symbol	Interpretation	Units	Value/Range*
S	Sediment water	Cm	-
V	vegetation biomass	g m^{-2}	-
T	Time	Day	-
X, Y	Space	M	-
A	Maximal growth rate of the sediment water (layer) at $S = 0$	cm day^{-1}	(0, 0.01]
S_m	Maximal thickness of the sediment water (layer)	Cm	5
L	specific sediment water loss due to evaporation	day^{-1}	0.05
P	Uptake of the sediment water	m^4 g^{-2} day^{-1}	0.3
H	Conversion of water uptake into vegetation biomass	g m^{-2} cm^{-1}	10
M	Mortality of the vegetation biomass	day^{-1}	0.02
U	Movement of the sediments along the downslope direction on hillslopes	m day^{-1}	10 or 0.001
D_S	Diffusive coefficient of sediment water	m^2 day^{-1}	0.2
D_V	Plant dispersal	m^2 day^{-1}	0.01

* A group of feasible values or ranges of the parameters are given referring to former empirical or theoretical studies in the literature [7–9, 21, 36–38].

diffusion coefficient of plant dispersal. The detailed information of the parameters and variables used in (1a) and (1b), such as ecological interpretation, units, and values/ranges, is presented in Table 1.

3. Conditions for Vegetation Pattern Formation

For determining whether the vegetation patterns can form in the considered ecological system, analysis of Turing instability is performed. Via analysis of Turing instability, the conditions for occurrence of spatially symmetry-breaking patterns (also called Turing patterns) can be found. According to the literature, two steps are taken for obtaining the conditions of Turing instability [8, 33, 34]. First, linear stability analysis is carried out on the nonspatial system to find a stable homogeneous stationary state. Second, spatially heterogeneous perturbations are made at the stable stationary state and the dynamic trend of the system is observed: if the perturbations diverge, the system will develop into a new, spatially patterned state.

For ecological significance, the dynamics of (1a) and (1b) are considered in the region $S \geq 0, V \geq 0$ that is of interest. Setting the space derivatives in (1a) and (1b) equal to zero, the nonspatial system is obtained. Then solving the equations obtained by letting time derivatives be zero, three spatially homogeneous stationary states can be got:

$$(S_0, V_0): \left(\frac{AS_m}{A + LS_m}, 0\right); \tag{2a}$$

$$(S_+, V_+): \left(\frac{A + \sqrt{A^2 - 4\left(A/S_m + L\right)\left(M^2/H^2P\right)}}{2\left(A/S_m + L\right)}, \frac{2\left(M/HP\right)\left(A/S_m + L\right)}{A + \sqrt{A^2 - 4\left(A/S_m + L\right)\left(M^2/H^2P\right)}}\right); \tag{2b}$$

$$(S_-, V_-): \left(\frac{A - \sqrt{A^2 - 4\left(A/S_m + L\right)\left(M^2/H^2P\right)}}{2\left(A/S_m + L\right)}, \frac{2\left(M/HP\right)\left(A/S_m + L\right)}{A - \sqrt{A^2 - 4\left(A/S_m + L\right)\left(M^2/H^2P\right)}}\right). \tag{2c}$$

The stationary state (S_0, V_0) suggests the state of no vegetation and bare ground. This state is without vegetation pattern formation and will not be considered. When $A^2H^2PS_m - 4(A + LS_m)M^2 > 0$, the stationary states (S_+, V_+) and (S_-, V_-) exist. In order to determine the linear stability of these two stationary states, linear stability analysis is performed as per the method of Jacobian matrix. The Jacobian matrix associated with the nonspatial system at any point (S, V) is

$$J_{(S,V)} = \begin{pmatrix} -\frac{A}{S_m} - L - PV^2 & -2PSV \\ HPV^2 & 2HPSV - M \end{pmatrix}. \tag{3}$$

Substituting the expressions of the stationary states into matrix (3) and calculating the corresponding eigenvalues, according to the signs of the two eigenvalues, the linear stability of the stationary states can be determined: if the two eigenvalues both show negative real part, it means stable stationary state; if one eigenvalue has positive real part, unstable stationary state is suggested. Straight calculation according to the above steps gets that (S_+, V_+) is always unstable, whereas (S_-, V_-) can be stable to homogenous perturbations. That means (S_-, V_-) is the stable homogeneous stationary state.

The heterogeneous perturbations at (S_-, V_-) are then performed to determine the conditions of Turing instability. The perturbation equations are expressed as

$$S(X, Y, T) = S_- + s(X, Y, T), \tag{4a}$$

$$V(X, Y, T) = V_- + v(X, Y, T), \tag{4b}$$

where s and v are small heterogeneous perturbations of sediment water and vegetation biomass.

Substituting the perturbation Eq. (4a) and (4b) into Eq. (1a) and (1b) yields

$$\frac{\partial s}{\partial T} = a_{11}s + a_{12}v + U\frac{\partial s}{\partial X} + D_S\left(\frac{\partial^2 s}{\partial X^2} + \frac{\partial^2 s}{\partial Y^2}\right) + o(s,v), \tag{5a}$$

$$\frac{\partial v}{\partial T} = a_{21}s + a_{22}v + D_V\left(\frac{\partial^2 v}{\partial X^2} + \frac{\partial^2 v}{\partial Y^2}\right) + o(s,v), \tag{5b}$$

where a_{ij} is given by

$$\begin{aligned} a_{11} &= -\frac{A}{S_m} - L - PV_-^2, \\ a_{12} &= -2\frac{M}{H}, \\ a_{21} &= HPV_-^2, \\ a_{22} &= M, \end{aligned} \tag{6}$$

and $o(s, v)$ is the high order terms of s or v.

The high order terms can be ignored when the perturbations s and v remain close to zero. Expanding s and v in Fourier space gives the following form of the perturbations [8, 34]:

$$s(X,Y,T) = \overline{s}(T)\, e^{i(k_1 X + k_2 Y)}, \tag{7a}$$

$$v(X,Y,T) = \overline{v}(T)\, e^{i(k_1 X + k_2 Y)}. \tag{7b}$$

In (7a) and (7b), $\overline{s}$ and $\overline{v}$ are only dependent on time, e is the natural exponential, i equals $\sqrt{-1}$, and k_1 and k_2 are the wavenumbers of the perturbations along the X-axis direction and Y-axis direction.

Substituting (7a) and (7b) into (5a) and (5b) results in

$$\frac{d\overline{s}}{dt} = \left(a_{11} + iUk_1 - D_S\left(k_1^2 + k_2^2\right)\right)\overline{s} + a_{12}\overline{v}, \tag{8a}$$

$$\frac{d\overline{v}}{dt} = a_{21}\overline{s} + \left(a_{22} - D_V\left(k_1^2 + k_2^2\right)\right)\overline{v}, \tag{8b}$$

The occurrence of the Turing instability is determined by whether the dynamic system (8a) and (8b) is diverse with the perturbations $\overline{s}$ and $\overline{v}$ [8]. Therefore, based on the Jacobian matrix of (8a) and (8b),

$$J = \begin{pmatrix} a_{11} + iUk_1 - D_S k^2 & a_{12} \\ a_{21} & a_{22} - D_V k^2 \end{pmatrix}, \tag{9}$$

where $k^2 = (k_1^2 + k_2^2)$, the following characteristic equation is obtained:

$$\lambda^2 - \left(a_{11} + a_{22} + iUk_1 - \left(D_S + D_V\right)k^2\right)\lambda + \left(a_{11} + iUk_1 - D_S k^2\right)\left(a_{22} - D_V k^2\right) - a_{12}a_{21} = 0. \tag{10}$$

Solving (10), the dispersion relation is got as follows:

$$\lambda(k_1,k_2) = \frac{1}{2}\left(a_{11} + a_{22} + iUk_1 - \left(D_S + D_V\right)k^2 + \sqrt{\alpha + i\beta}\right), \tag{11}$$

in which

$$\alpha = \left(a_{11} - a_{22} - \left(D_S - D_V\right)k^2\right)^2 + 4a_{12}a_{21} - U^2k_1^2, \tag{12a}$$

$$\beta = 2Uk_1\left(a_{11} - a_{22} - \left(D_S - D_V\right)k^2\right). \tag{12b}$$

The real part and image part of $\lambda(k_1, k_2)$ can be determined via straightforward manipulation on (11):

$$\mathrm{Re}\left(\lambda_\pm(k_1,k_2)\right) = \frac{1}{2}\left(a_{11} + a_{22} - \left(D_S + D_V\right)k^2 \pm \frac{1}{\sqrt{2}}\sqrt{\sqrt{\alpha^2 + \beta^2} + \alpha}\right), \tag{13a}$$

$$\mathrm{Im}\left(\lambda_\pm(k_1,k_2)\right) = \frac{1}{2}\left(Uk_1 \pm \frac{1}{\sqrt{2}}\mathrm{sign}(\beta)\sqrt{\sqrt{\alpha^2 + \beta^2} - \alpha}\right). \tag{13b}$$

As described previously, the emergence of Turing instability and vegetation pattern formation must satisfy the condition that the stationary state is stable to spatially homogeneous perturbations but unstable to spatially heterogeneous perturbations. According to linear stability analysis, spatially stable stationary state is found. Therefore, the divergence of the heterogeneous perturbations at the stable stationary state (i.e., system (8a) and (8b) diverges) determines the criterion for Turing instability. That means

$$\mathrm{Re}\left(\lambda_+(k_1,k_2)\right) > 0 \tag{14}$$

for any k_1 or k_2 not equal to zero. Condition (14) provides the parametric condition for the vegetation pattern formation of the system governed by (1a) and (1b).

4. Numerical Results

Numerical simulations are carried out via discretizing the partial differential equations (1a) and (1b). Upwinding difference scheme is applied to the advection term and finite difference approximation to the diffusion term and an explicit Euler method for the time integration with a time stepsize $\Delta T = 0.02$ [9, 35]. The scale of space and time is averaged for the Euler method. The spatial vegetation patterns are plotted in a rectangle domain representing 100×100 cells, with the positive X-axis direction as the downslope direction. In all numerical simulations, periodic boundary conditions are employed [7]. Random perturbations around the stable stationary state (S_-, V_-) are adopted as the initial conditions [35].

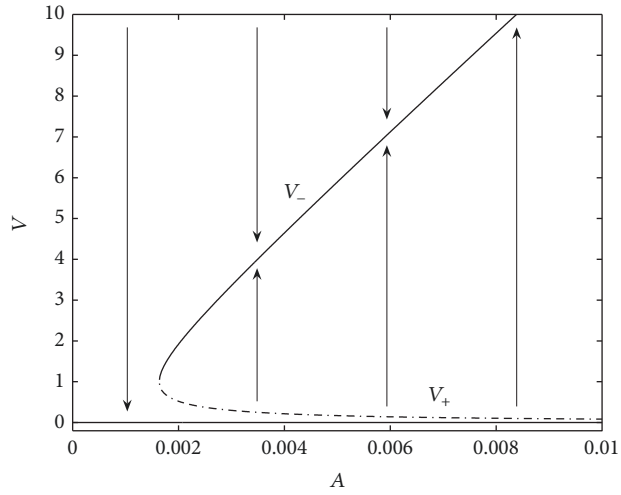

Figure 1: Bifurcation diagram for variable V and parameter A. The solid curve describes the stable stationary state V_- and the dashed curve describes the unstable stationary state V_+. The arrows denote the state which the system tends to approach.

The values of parameters applied for the numerical simulations are shown in Table 1. These parameter values are given referring to the literature, in order to represent the conditions close to reality. Parameters A and U are used as varying parameters, since the two parameters demonstrate main properties of sediment deposition process on hillslopes. Simultaneously, the values of parameters A and U are also restricted by condition (14). Two types of vegetation patterns are simulated: (a) banded vegetation patterns generated when U =10 and (b) labyrinth and gapped vegetation patterns generated when U is a small value. For better showing the patterns, space stepsize is set as 0.5 for banded patterns and as 1 for labyrinth and gapped patterns.

Variation of parameter A, the growth rate of sediment layer, represents the change of water input to the ecological system considered. Figure 1 shows how the system responds to the change of water input in V-A bifurcation diagram. When $A < A_1 = 1.64 \times 10^{-3}$, the system shows state of bare ground. This value A_1 is also the threshold point where a sudden shift happens between the vegetated state and the state of bare ground. When $A \geq A_1$, a saddle-node bifurcation results in two branches of stationary states, V_- and V_+: V_- is stable and V_+ is unstable. The increase of V_- and the decrease of V_+ with the parameter A suggest that more supply of sediment water can conduce to development and stabilization of vegetation in the water-limited ecosystems.

Before the pattern simulations are performed, the value range of selected varying parameter A for pattern formation is determined. The Turing instability is demonstrated in Figure 2. Figure 2(a) exhibits the graph of $\mathrm{Re}(\lambda_+(k_1, k_2))$, showing that when $k_1 = 28$ and $k_2 = 1$, $\mathrm{Re}(\lambda_+(k_1, k_2))$ reaches the maximum value as 0.013. This suggests the occurrence of Turing instability under the corresponding parametric conditions. Figure 2(b) demonstrates the change of $\max(\mathrm{Re}(\lambda_+(k_1, k_2)))$ with the variation of parameter A. It is found that the region for the occurrence of Turing instability is $1.64 \times 10^{-3} < A < 8.87 \times 10^{-3}$.

Figure 3 shows the region diagram corresponding to parameters A and U. In the region diagram, three areas are divided, namely, areas of no vegetation, patterned vegetation, and homogeneous vegetation, respectively. As the water input gradually increases, the system may go from no vegetation, through patterned vegetation, to homogeneous vegetation. Simultaneously, increase of U leads to larger patterned formation range, making the system stay in patterned formation zone longer.

Referring to Rietkerk et al. [9], the parameter U can be given at U=10, representing explicit sediment flux on hillslopes. In such case, the influence of sediment water diffusion on the vegetation pattern formation is minor since the value of D_S is relatively too small. According to Figure 2, when U=10, the parameter A ranges from 1.64×10^{-3} to 8.87×10^{-3}.

The downslope flux of sediments leads to the formation of regular banded vegetation patterns on planar hillslopes, as shown in Figure 4. The vegetation stripes (Figure 4(a)) will gradually develop into parallel typical vegetation bands (Figure 4(b)). These vegetation bands are perpendicular to the downslope direction and will migrate upslope with time.

The main characteristic of banded vegetation patterns is the wavelength. As shown in Figure 5, power spectrum analysis on the pattern of Figure 4(b) is carried out and shows the dominant wavenumber of this pattern. The dominant wavenumber is in agreement with that expected by the analytical dispersion relation shown in Figure 5(b). Note that the product of wavenumber and wavelength equals 2π. The result suggests that the wavelength of banded vegetation pattern is inherently determined by maximum dispersion rate of heterogeneous perturbations at the homogeneous stationary state.

As the value of parameter A varies, the wavelength of banded pattern will change. The change of wavelength with A describes how the water input specifically affects the spatial distribution of vegetation biomass. Figure 6 shows the relationship between the wavelength and parameter A. When A has smaller values, the wavelength varies greatly as A increases; whereas when A keeps at higher values, the change of the wavelength tends to be slow. This implies that the patterned vegetation is sensitive to the change of sediment water when it is very drought but becomes stable when the sediment water is relatively sufficient.

When U keeps at tiny value, more complex vegetation patterns may form. The tiny U means that the sediments on the hillslopes barely move and suggests the stabilization of the sediment layer. In order to simulate the formation of vegetation patterns in such case, the parameter U is given at U=0.001. According to Figure 3, corresponding to U=0.001, the occurrence of pattern formation of the system needs that the value of parameter A ranges from 1.64×10^{-3} to 1.71×10^{-3}.

Figure 7 describes the formation of labyrinth vegetation patterns when $A = 1.65 \times 10^{-3}$. When T is less than 3000 days, the vegetation pattern is comprised of spots and small stripes (Figure 7(a)). The vegetation spots will gradually

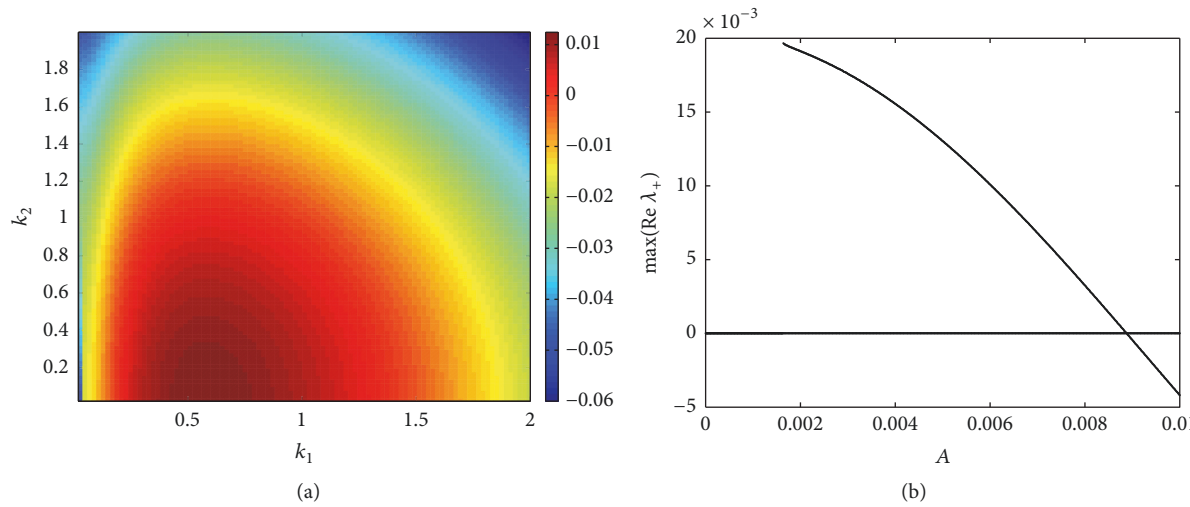

FIGURE 2: (a) Graph of $\mathrm{Re}(\lambda_+(k_1, k_2))$ when $A = 0.005$ and (b) change of $\max(\mathrm{Re}(\lambda_+(k_1, k_2)))$ with the variation of parameter A. $U = 10$.

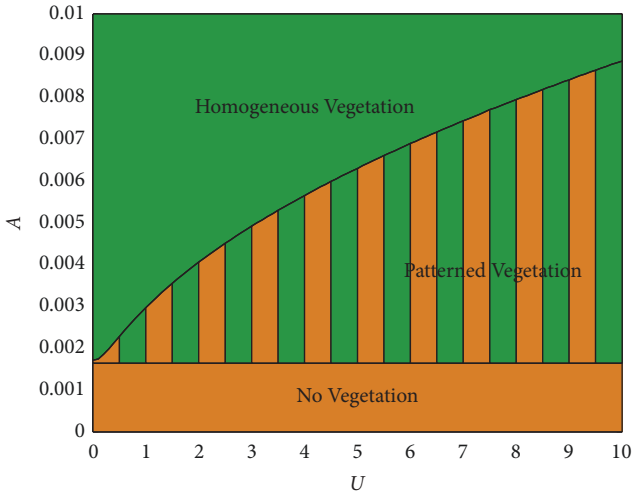

FIGURE 3: Region diagram corresponding to parameters A and U. Three areas are divided: areas of no vegetation, patterned vegetation, and homogeneous vegetation.

disappear and eventually the labyrinthic stripes dominate. Figure 7(b) shows the formed labyrinth vegetation pattern at $T = 10000$.

As the value of parameter A gradually increases, the labyrinth vegetation patterns will fade out and the gapped vegetation pattern will develop. Figure 8 shows two gapped vegetation patterns. The contrast between Figures 8(a) and 8(b) demonstrates that increase of sediment water input leads to the shrink of dot gaps. This implies the gradual developing process from patterned vegetation into homogeneous vegetation provided that the water resource becomes sufficient.

Inferentially, transitional patterns must exist between Figures 7 and 8. As shown in Figure 9, a transitional vegetation pattern between labyrinth pattern and gapped pattern is presented. This transitional pattern can be also regarded as spatial mixture of two distinct patterns of Figures 7 and 8.

5. Discussion

As widely recognized, the interactions between water and biomass are the key mechanisms which drive formation of vegetation patterns in water-limited ecosystems [6, 8]. Different from the former studies in literature, this research focuses on the vegetation pattern formation in the case where the topsoil is severely disturbed or removed. The water resource supplying for such system is from the water in the deposited sediment layer. Attributed to the interactions between vegetation biomass and sediment water, self-organization of vegetation patterns can take place.

Based on the Klausmeier's approach [7] and the interactions between vegetation biomass and sediment water, a nonlinear spatiotemporal model is established to investigate the vegetation pattern formation in the ecological system described above. The results obtained in the above sections demonstrate the formation of two cases of vegetation patterns for the considered system: banded vegetation pattern when U has high values (such as 10) and labyrinth and gapped vegetation patterns when U keeps tiny (such as 0.001).

Banded vegetation patterns are the most important patterns on sloped terrains [5, 7, 16, 39, 40]. Due to the unidirectional sheet flow on sloped terrains and the competition between plants for water resource, the lateral growth of vegetation stripes is prevented and parallel vegetation bands are self-organized [39]. Specifically, the banded pattern formation described in this research involves one important geomorphic process, sediment deposition process on hillslopes. Such pattern formation was also described by Bryan and Oostwoud Wijdenes [30].

For the banded vegetation patterns, wavelength is the most important characteristic. The analysis on the wavelength of banded patterns in this research suggests that the wavelength decreases in a nonlinear function as the input of sediment water increases. This result is in agreement with the description of the relationship between the water input and the bands wavelength obtained by Klausmeier [7], Sherratt [41], and Borthagaray et al. [16]. For grasses, the wavelengths

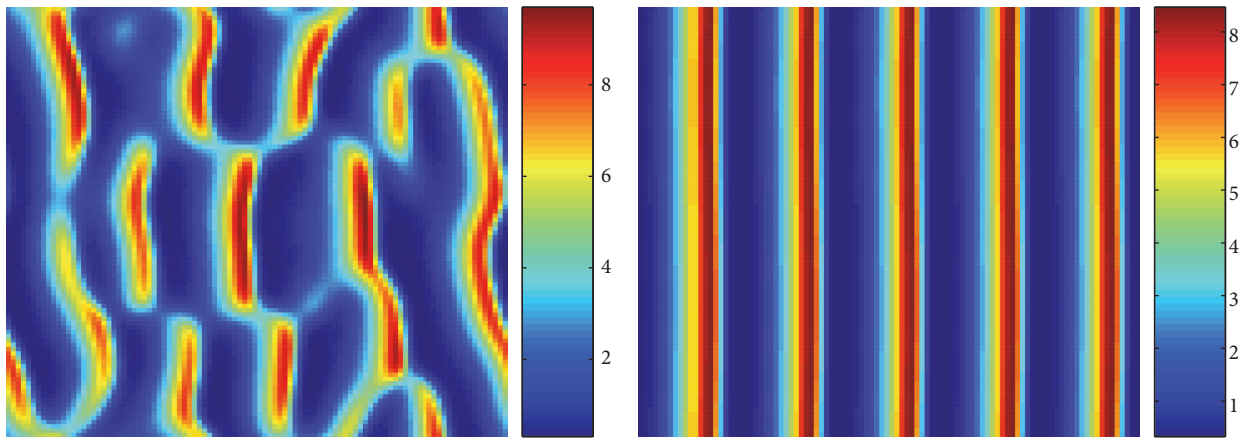

Figure 4: Self-organization of a regular banded vegetation pattern on planar hillslopes when $A = 6.00 \times 10^{-3}$. (a) $T = 1000$; (b) $T = 20000$. The downslope direction is from left to right in each graph and in the pattern graphs below.

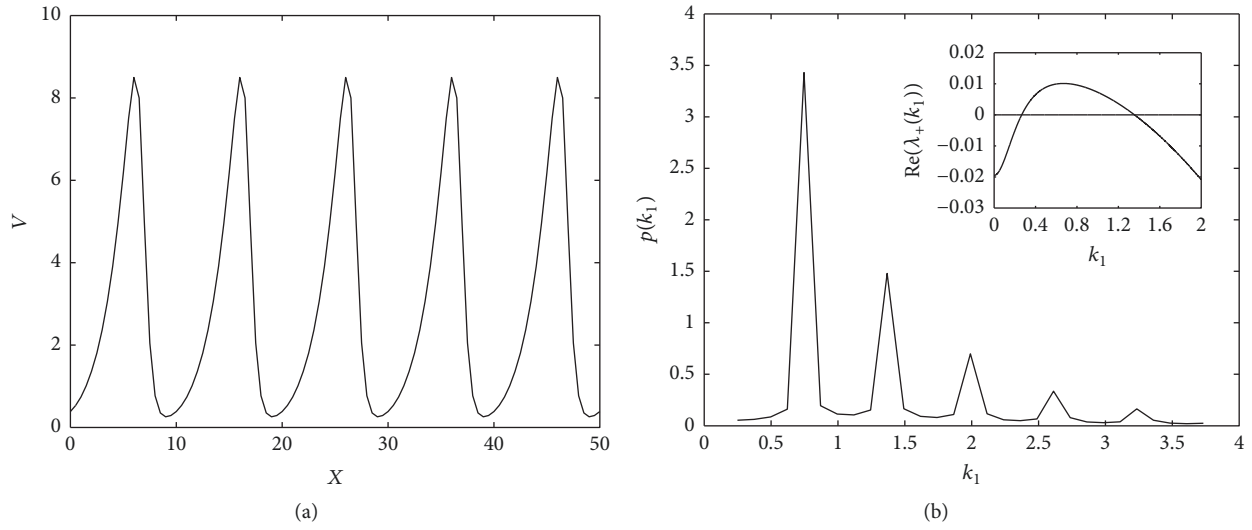

Figure 5: (a) Spatial wave of plant biomass, obtained by a cross-section of Figure 4(b); (b) power spectrum analysis for Figure 5(a), where the inner graph is the corresponding dispersion relation for Figure 4, plotted using (13a).

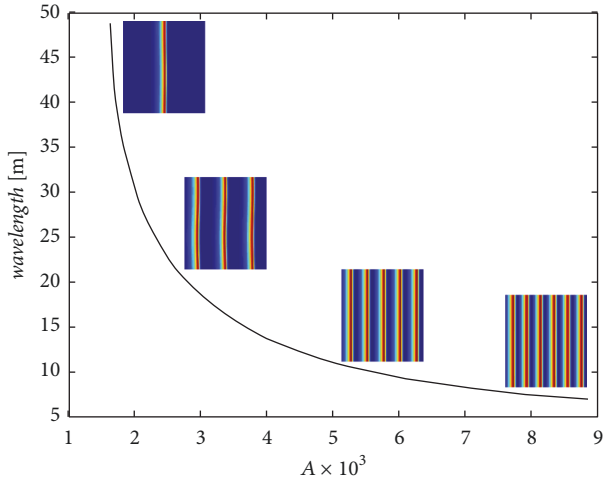

Figure 6: The relationship between the wavelength of banded vegetation patterns and the parameter A.

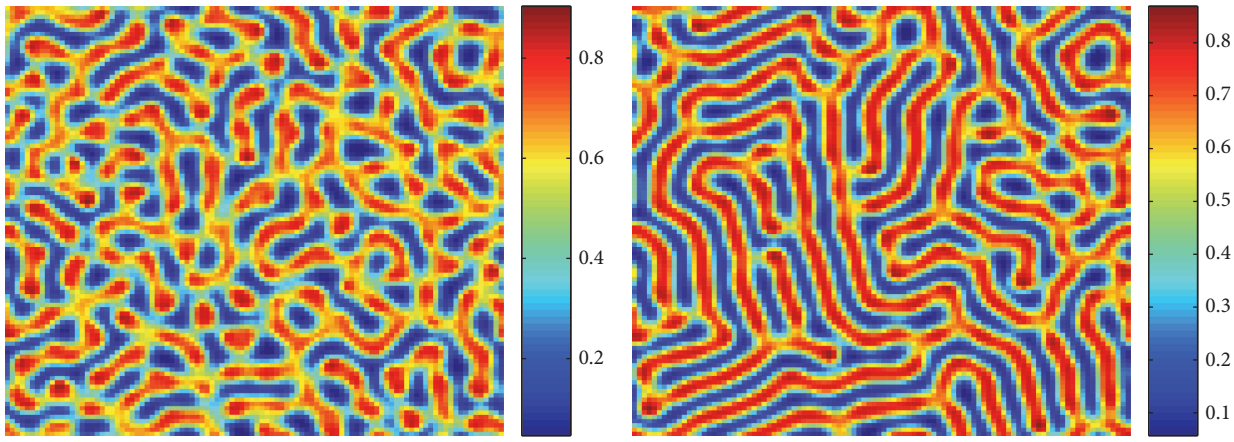

Figure 7: Formation of labyrinth vegetation pattern. $A = 1.65 \times 10^{-3}$. (a) T=2000; (b) T=10000.

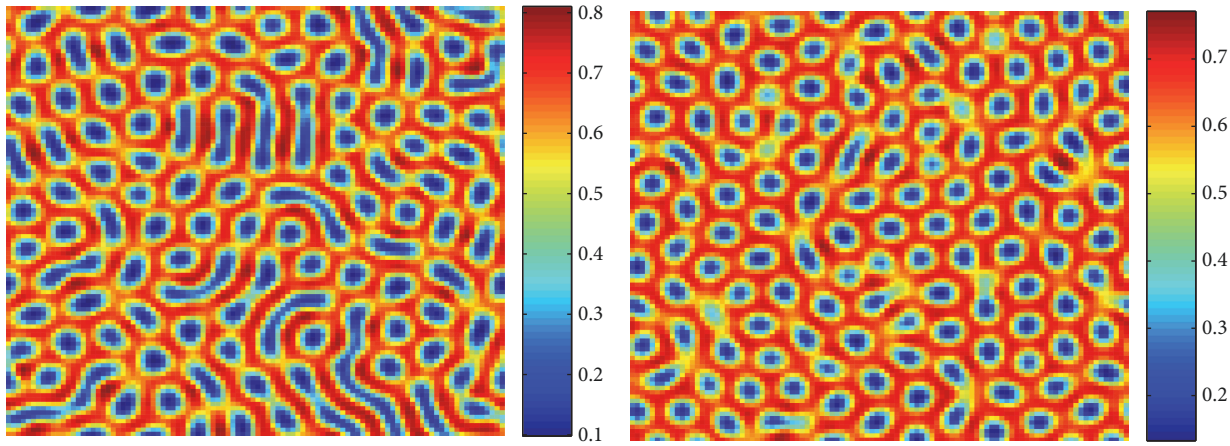

Figure 8: Two gapped vegetation patterns for the system. (a) $A = 1.68 \times 10^{-3}$; (b) $A = 1.70 \times 10^{-3}$. T=10000.

are observed to be often ranging from 10m to 100m [5, 42, 43]. Comparable to that, the wavelength range obtained in this research is from 7m to 50m. It implies small-scale grass bands for the obtained results, in agreement with the description in literature [30, 31].

When U takes small values, it implies the stabilization of deposited sediment layer. In such case, labyrinth and gapped vegetation patterns are predicted. Since spatial distribution of vegetation biomass is mainly determined by the diffusive movement of water in sediment layer, the pattern formation in this case is similar to that described in Rietkerk et al. [9] and Meron et al. [44]. Moreover, the changing process of vegetation patterns with the increase of water input described in this research also accords with that described in Rietkerk et al. [9] and Meron et al. [44].

Since the sediments deposited on the eroded ground provide a new interface for vegetation growth, the self-organization of vegetation patterns studied in this research implies an ecological restoration process on the degraded lands. This is different from the models established by descriptions in literature that vegetation pattern formation represents vegetation degradation which results from over-grazing, trampling, or drought [8, 9, 45]. As described in Bryan and Brun [31], the formation of patterned vegetation of this research may represent a first stage in the recolonization of severely degraded surfaces, rather than a late stage in vegetation deterioration.

6. Conclusions

In this research, a theoretical and numerical investigation is performed to study the vegetation pattern formation on severely degraded land. The original soil layer is considered as destroyed by soil erosion, and the sediment layer deposited on the ground is considered to provide an environment to contain water and provide a water resource for vegetation growth. On the basis of the interactions between vegetation biomass and sediment water, a nonlinear spatiotemporal model is established to describe the pattern formation in such ecological system.

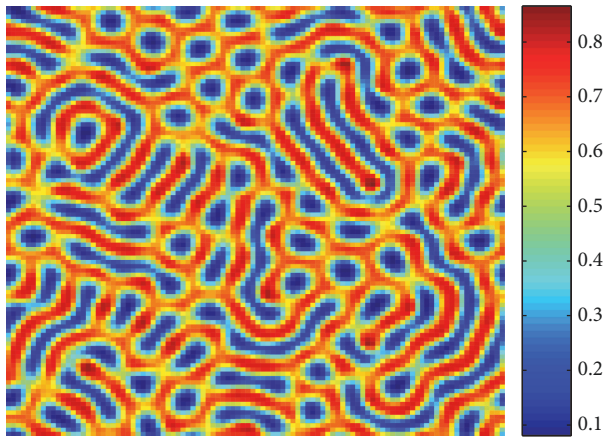

Figure 9: Transitional vegetation pattern between the labyrinth pattern and the gapped pattern. $A = 1.67 \times 10^{-3}$. T=10000.

Via the analysis of Turing instability, the conditions for pattern formation are determined. Numerical simulations for the pattern formation are performed under the conditions determined. In the simulations, a group of feasible values of the system parameters are taken from the literature, representing the conditions close to reality. With the employment of the model developed, the simulations demonstrate that two cases of vegetation patterns can be self-organized, i.e., the banded vegetation patterns on hillslopes when the movement of sediments appears, and the labyrinth and gapped vegetation patterns when the sediment layer approaches stabilization. Comparing the characteristics of the vegetation patterns of this research with that available in the literature, great similarity of pattern formation is shown.

Referring to the literature, the theoretical model in this research can be further analyzed with the application of other mathematical tools. For example, multiple scale analysis can show the bifurcation behavior of the vegetation dynamics as a function of parameters [46]. It should be noticed that the present theoretical model is a developed version of the Klausmeier model, which has been detailedly and systemically explored in literature. From the previous study on the Klausmeier model [18], bifurcation dynamics and amplitude equations can be applied in this research to know pattern selection and pattern transition of the vegetation under the influence of sediment water on severely degraded land. Since the storage of sediment water is closely related to rainfall rate, it can be deduced that rainfall plays an important role in vegetation pattern selection. The methods as described in Consolo et al. [47] and Li et al. [48] also provide effective tools for analyzing periodic solutions and pattern migration of the system of the vegetation and sediment water, which should be further investigated in the future work with the utilization of advanced mathematical tools.

Different from the significance of patterned vegetation described in former research works, the patterned vegetation in this research describes recovery of degraded ecological systems. This investigation provides a theoretical comprehension about the natural restoration of vegetation on severely degraded lands.

Data Availability

The data of numerical results are generated during the study.

Conflicts of Interest

The authors declare no conflicts of interest.

Acknowledgments

This research was financed by the National Water Pollution Control and Treatment Science and Technology Major Project (No. 2015ZX07204-007 and No. 2017ZX07101-002), the National Natural Science Foundation of China (No. 11802093), and the Fundamental Research Funds for the Central Universities (No. JB2017069).

References

[1] R. O. Slatyer, "Methodology of a water balance study conducted on a desert woodland (Acacia aneura F. Muell) community in central Australia," in *Plant-Water Relationships in Arid and Semi-Arid Conditions*, vol. 16, pp. 15–25, UNESCO Arid Zone Research, 1961.

[2] L. P. White, "Vegetation stripes on sheet wash surfaces," *Journal of Ecology*, vol. 59, pp. 615–622, 1971.

[3] D. Dunkerley and K. Brown, "Runoff and runon areas in a patterned chenopod shrubland, arid western New South Wales, Australia: characteristics and origin," *Journal of Arid Environments*, vol. 30, no. 1, pp. 41–55, 1995.

[4] J. M. Thiery, J. D'Herbes, and C. Valentin, "A model simulating the genesis of banded vegetation patterns in niger," *Journal of Ecology*, vol. 83, no. 3, pp. 497–507, 1995.

[5] C. Valentin, J. M. D'Herbès, and J. Poesen, "Soil and water components of banded vegetation patterns," *Catena*, vol. 37, no. 1-2, pp. 1–24, 1999.

[6] F. Borgogno, P. D'Odorico, F. Laio, and L. Ridolfi, "Mathematical models of vegetation pattern formation in ecohydrology," *Reviews of Geophysics*, vol. 47, no. 1, 2009.

[7] C. A. Klausmeier, "Regular and irregular patterns in semiarid vegetation," *Science*, vol. 284, no. 5421, pp. 1826–1828, 1999.

[8] R. HilleRisLambers, M. Rietkerk, F. van den Bosch, H. H. Prins, and H. de Kroon, "Vegetation Pattern Formation in Semi-Arid Grazing Systems," *Ecology*, vol. 82, no. 1, p. 50, 2001.

[9] M. Rietkerk, M. C. Boerlijst, F. van Langevelde et al., "Self-organization of vegetation in arid ecosystems," *The American Naturalist*, vol. 160, no. 4, pp. 524–530, 2002.

[10] E. Gilad, J. von Hardenberg, A. Provenzale, M. Shachak, and E. Meron, "Ecosystem engineers: from pattern formation to habitat creation," *Physical Review Letters*, vol. 93, no. 9, article no. 098105, 2004.

[11] J. A. Ludwig, B. P. Wilcox, D. D. Breshears, D. J. Tongway, and A. C. Imeson, "Vegetation patches and runoff–erosion as interacting ecohydrological processes in semiarid landscapes," *Ecology*, vol. 86, no. 2, pp. 288–297, 2005.

[12] N. Barbier, P. Couteron, J. Lejoly, V. Deblauwe, and O. Lejeune, "Self-organized vegetation patterning as a fingerprint of climate and human impact on semi-arid ecosystems," *Journal of Ecology*, vol. 94, no. 3, pp. 537–547, 2006.

[13] S. Thompson, G. Katul, and S. M. McMahon, "Role of biomass spread in vegetation pattern formation within arid ecosystems," *Water Resources Research*, vol. 44, no. 10, 2008.

[14] S. Kéfi, M. B. Eppinga, P. C. de Ruiter, and M. Rietkerk, "Bistability and regular spatial patterns in arid ecosystems," *Theoretical Ecology*, vol. 3, no. 4, pp. 257–269, 2010.

[15] J. von Hardenberg, A. Y. Kletter, H. Yizhaq, J. Nathan, and E. Meron, "Periodic versus scale-free patterns in dryland vegetation," *Proceedings of the Royal Society B Biological Science*, vol. 277, no. 1688, pp. 1771–1776, 2010.

[16] A. I. Borthagaray, M. A. Fuentes, and P. A. Marquet, "Vegetation pattern formation in a fog-dependent ecosystem," *Journal of Theoretical Biology*, vol. 265, no. 1, pp. 18–26, 2010.

[17] J. von Hardenberg, E. Meron, M. Shachak, and Y. Zarmi, "Diversity of vegetation patterns and desertification," *Physical Review Letters*, vol. 87, no. 19, article no. 198101, 2001.

[18] G. Sun, L. Li, and Z. Zhang, "Spatial dynamics of a vegetation model in an arid flat environment," *Nonlinear Dynamics*, vol. 73, no. 4, pp. 2207–2219, 2013.

[19] J. Lu and H. Dai, "Numerical modeling of pollution transport in flexible vegetation," *Applied Mathematical Modelling*, vol. 64, pp. 93–105, 2018.

[20] G.-Q. Sun, C.-H. Wang, L.-L. Chang, Y.-P. Wu, L. Li, and Z. Jin, "Effects of feedback regulation on vegetation patterns in semi-arid environments," *Applied Mathematical Modelling: Simulation and Computation for Engineering and Environmental Systems*, vol. 61, pp. 200–215, 2018.

[21] K. Descheemaeker, J. Nyssen, J. Rossi et al., "Sediment deposition and pedogenesis in exclosures in the Tigray highlands, Ethiopia," *Geoderma*, vol. 132, no. 3-4, pp. 291–314, 2006.

[22] H. Strunk, "Soil degradation and overland flow as causes of gully erosion on mountain pastures and in forests," *Catena*, vol. 50, no. 2-4, pp. 185–198, 2003.

[23] R. Bou Kheir, O. Cerdan, and C. Abdallah, "Regional soil erosion risk mapping in Lebanon," *Geomorphology*, vol. 82, no. 3-4, pp. 347–359, 2006.

[24] Y. Cantón, A. Solé-Benet, J. de Vente et al., "A review of runoff generation and soil erosion across scales in semiarid south-eastern Spain," *Journal of Arid Environments*, vol. 75, no. 12, pp. 1254–1261, 2011.

[25] L. Martín-Fernández and M. Martínez-Núñez, "An empirical approach to estimate soil erosion risk in Spain," *Science of the Total Environment*, vol. 409, no. 17, pp. 3114–3123, 2011.

[26] Y. Le Bissonnais, B. Renaux, and H. Delouche, "Interactions between soil properties and moisture content in crust formation, runoff and interrill erosion from tilled loess soils," *Catena*, vol. 25, no. 1-4, pp. 33–46, 1995.

[27] D. Robinson and C. Phillips, "Crust development in relation to vegetation and agricultural practice on erosion susceptible, dispersive clay soils from central and southern Italy," *Soil & Tillage Research*, vol. 60, no. 1-2, pp. 1–9, 2001.

[28] M. Neave and S. Rayburg, "A field investigation into the effects of progressive rainfall-induced soil seal and crust development on runoff and erosion rates: the impact of surface cover," *Geomorphology*, vol. 87, no. 4, pp. 378–390, 2007.

[29] X. Hu, L. Liu, S. Li, Q. Cai, Y. Lü, and J. Guo, "Development of soil crusts under simulated rainfall and crust formation on a loess soil as influenced by polyacrylamide," *Pedosphere*, vol. 22, no. 3, pp. 415–424, 2012.

[30] R. B. Bryan and D. Oostwoud Wijdenes, "Field and laboratory experiments on the evolution of microsteps and scour channels on low-angle slopes," in *Functional Geomorphology: Landform Analysis and Models*, K. H. Schmidt and J. De Ploey, Eds., vol. 23 of *Catena Supplement*, pp. 1–29, Catena-Verlag, Reiskirchen, Germany, 1992.

[31] R. Bryan and S. Brun, "Laboratory experiments on sequential scour/deposition and their application to the development of banded vegetation," *Catena*, vol. 37, no. 1-2, pp. 147–163, 1999.

[32] J. Puigdefabregas, A. Sole, L. Gutierrez, G. Del Barrio, and M. Boer, "Scales and processes of water and sediment redistribution in drylands: results from the Rambla Honda field site in Southeast Spain," *Earth-Science Reviews*, vol. 48, no. 1-2, pp. 39–70, 1999.

[33] A. M. Turing, "The chemical basis of morphogenesis," *Philosophical Transactions of the Royal Society B: Biological Sciences*, vol. 237, no. 641, pp. 37–72, 1952.

[34] Q. Ouyang, *Pattern Formation in Reaction-Diffusion Systems*, Shanghai science and technology education press, Shanghai, China, 2000.

[35] G. Sun, L. Li, Z. Jin, and B. Li, "Pattern formation in a spatial plant-wrack model with tide effect on the wrack," *Journal of Biological Physics*, vol. 36, no. 2, pp. 161–174, 2010.

[36] Y. Avnimelech, G. Ritvo, L. E. Meijer, and M. Kochba, "Water content, organic carbon and dry bulk density in flooded sediments," *Aquacultural Engineering*, vol. 25, no. 1, pp. 25–33, 2001.

[37] L. Mabit, A. Klik, M. Benmansour, A. Toloza, A. Geisler, and U. Gerstmann, "Assessment of erosion and deposition rates within an Austrian agricultural watershed by combining ^{137}Cs, ^{210}Pb$_{ex}$ and conventional measurements," *Geoderma*, vol. 150, no. 3-4, pp. 231–239, 2009.

[38] J. C. Ritchie, V. L. Finney, K. J. Oster, and C. A. Ritchie, "Sediment deposition in the flood plain of Stemple Creek Watershed, northern California," *Geomorphology*, vol. 61, no. 3-4, pp. 347–360, 2004.

[39] P. M. Saco, G. R. Willgoose, and G. R. Hancock, "Eco-geomorphology of banded vegetation patterns in arid and semi-arid regions," *Hydrology and Earth System Sciences*, vol. 11, no. 6, pp. 1717–1730, 2007.

[40] M. Rietkerk and J. van de Koppel, "Regular pattern formation in real ecosystems," *Trends in Ecology & Evolution*, vol. 23, no. 3, pp. 169–175, 2008.

[41] J. A. Sherratt, "An analysis of vegetation stripe formation in semi-arid landscapes," *Journal of Mathematical Biology*, vol. 51, no. 2, pp. 183–197, 2005.

[42] M. Rietkerk, S. C. Dekker, P. C. de Ruiter, and J. van de Koppel, "Self-organized patchiness and catastrophic shifts in ecosystems," *Science*, vol. 305, no. 5692, pp. 1926–1929, 2004.

[43] J. A. Sherratt, "Pattern solutions of the Klausmeier Model for banded vegetation in semi-arid environments I," *Nonlinearity*, vol. 23, no. 10, pp. 2657–2675, 2010.

[44] E. Meron, E. Gilad, J. Von Hardenberg, M. Shachak, and Y. Zarmi, "Vegetation patterns along a rainfall gradient," *Chaos, Solitons & Fractals*, vol. 19, no. 2, pp. 367–376, 2004.

[45] M. Scheffer, J. Bascompte, W. A. Brock et al., "Early-warning signals for critical transitions," *Nature*, vol. 461, no. 7260, pp. 53–59, 2009.

[46] G. Sun, C. Wang, and Z. Wu, "Pattern dynamics of a Gierer–Meinhardt model with spatial effects," *Nonlinear Dynamics*, vol. 88, no. 2, pp. 1385–1396, 2017.

[47] G. Consolo, C. Currò, and G. Valenti, "Pattern formation and modulation in a hyperbolic vegetation model for semiarid

environments," *Applied Mathematical Modelling*, vol. 43, pp. 372–392, 2017.

[48] L. Li, Z. Jin, and J. Li, "Periodic solutions in a herbivore-plant system with time delay and spatial diffusion," *Applied Mathematical Modelling*, vol. 40, no. 7-8, pp. 4765–4777, 2016.